

AN OVERVIEW OF THE COLLECTIVE EFFECTS AND IMPEDANCE CALCULATION FOR THE EIC*

A. Blednykh[†], M. Blaskiewicz, D. Gassner, C. Hetzel, B. Lepore, B. Podobedov, V. Ranjbar, M. Sangroula, P. Thieberger, S. Verdu-Andres, G. Wang, Q. Wu
Brookhaven National Laboratory, Upton, NY, USA

Abstract

A new high-luminosity Electron Ion Collider (EIC) is under design at Brookhaven National Laboratory (BNL). Stable operation of the electron beam at average current of 2.5 A within 1100 bunches with a 7 mm bunch length is one of the challenging tasks in achieving an electron-proton luminosity of 10^{33} - 10^{34} cm⁻² sec⁻¹ range. Beam induced heating, short-range and long-range wakefield analysis is discussed for some of the vacuum components of the electron storage ring (ESR), the hadron storage ring (HSR) and the rapid cycling synchrotron (RCS) and as well as the impact of the collective effects on the beam stability.

INTRODUCTION

In this paper we discuss single- and multi-bunch effects of the electron and proton beams in the Electron Ion Collider (EIC) for the accelerator parameters presented in the EIC Conceptual Design Report [1]. The new electron injection scheme of the EIC consists of the electron polarized source, 400 MeV LINAC, the rapid cycling synchrotron (RCS) with a possible energy ramp from 400 MeV to 18 GeV and the electron storage ring (ESR), where the beam can be accelerated at 5 GeV, 10 GeV and 18 GeV energy. While the ion injection scheme is based on the present RHIC facility [2], which includes the proton polarized source, the 200 MeV LINAC, the booster, the Alternating Gradient Synchrotron (AGS) and the Hadron Storage Ring (HSR).

RCS

The RCS lattice has a hard Dynamic Aperture limit in dp/p of 1%. In order to keep below this, we limit our RMS dp/p to 2.5×10^{-3} . However, we are also bounded on the lower side of dp/p by collective instabilities. A modified version of TRANFT [3] was used to simulate coherent instabilities while ramping a single bunch in the rapid cycling synchrotron (RCS) from 400 MeV to 18 GeV. Simulations incorporated both long- and short-range wakefields although only broad-band impedances had an impact on beam dynamics.

These simulations have shown that longitudinal instabilities make it challenging to accumulate 28 nC per bunch at the injection energy of 400 MeV. For this reason, we plan on injecting 8x7 nC bunches and accelerating them to 1 GeV while maintaining a bunch energy deviation of 0.25% and squeezing the bunch length to 16 ps. This

should preserve the longitudinal emittance, while keeping the bunches above the microwave instability threshold.

At 1 GeV the bunches will be merged to form two 28 nC bunches. Merge simulation including collective and radiative effects yield a growth of 42% with a final $\sigma_r \sigma_E$ emittance of 2.27×10^{-4} eV-s from the individual 4×10^{-5} eV-s. The longitudinal instability results are also confirmed using the approximate formulas for the microwave instability thresholds less than $Z/n > 0.1 \Omega$ as can be seen in Fig. 1.

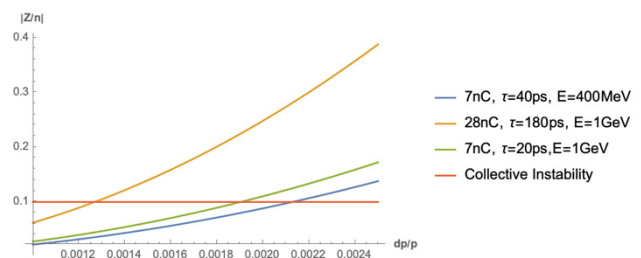


Figure 1: Plot of various Z/n estimated values for 7 nC RCS bunches at 400 MeV and 7nC and 28 nC bunches at 1 GeV versus dp/p with the assumed 0.1Ω collective instability threshold. We see at 1 GeV 28 nC bunches with 180 ps bunches are well above the longitudinal collective stability threshold.

HSR

Beam Screen

With the current RHIC beam pipe, the EIC hadron storage ring will be vulnerable to electron cloud instabilities and high resistive losses from beam-induced currents. The vacuum chamber of the EIC HSR SC magnets and their cold interconnects will be updated with a beam screen designed to present sufficiently low impedance and low secondary electron-emission yield (SEY) [4]. Our baseline solution – a high-conductivity copper-clad stainless-steel shell coated with low-SEY amorphous carbon – mirrors the screens developed for the Large Hadron Collider (LHC) [5] and the High Luminosity LHC (HL-LHC) [6]. One major difference between the EIC and LHC designs is that the EIC HSR beam screens will be cooled by direct thermal contact to the 4.55 K cold bore beam pipe. A particular challenge is the insertion of the screens through the beam pipe of the RHIC arc dipoles, with a significantly larger sagitta (48.5 mm over a total length of about 10 m) than the LHC ones (9 mm over 15 m). An R&D program is in place to develop, prototype and test the beam screen design.

* Work supported by Brookhaven Science Associates, LLC under Contract No. DE-SC0012704 with the U.S. Department of Energy.

[†] blednykh@bnl.gov

Crab Cavities

Transverse Crab cavities can lead to transverse coupled bunch instabilities. It is well known that higher order modes (HOMs) can be a problem but the fundamental mode responsible for the crabbing itself can lead to severe instabilities as well. An important point here is that the transverse impedance needs to be evaluated at the appropriate sideband of the coherent frequency, including any imaginary part. Figure 2 shows the growth rate of the transverse coupled bunch mode for a crab cavity system with an external $Q = 3 \times 10^6$ and no RF feedback. The green curve is the result from tracking many bunches with full transverse and RF dynamics. The red curve tracks a symmetric fill with ‘bunches’ consisting of two macro-particles at a fixed distance of $2\sigma_s$. Both these simulations put the entire crab wake in a single thin lens. The black curve is the solution of an analytic problem similar to the simple tracking but with the crab impedance uniformly distributed around the accelerator. The blue curve is the transverse resistance of the crab cavity scaled to a peak of 1. The large growth rates seen in the instabilities greatly broaden the transverse resistance. The instability can be cured by adding sufficient RF feedback to the crabbing RF system. The maximum loop delay is being developed but is of order 100 ns.

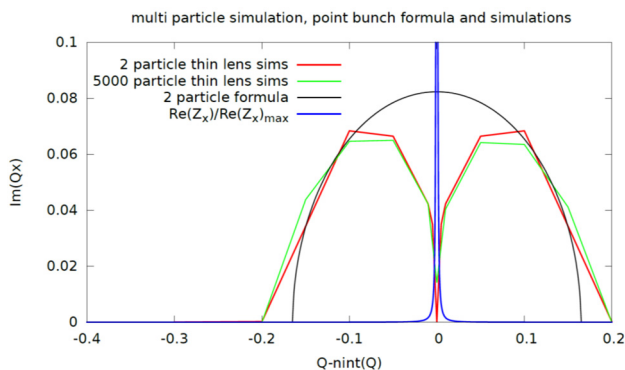


Figure 2: Imaginary part of the tune versus the non-integer part of the set tune for 3 different models of the instability due to the crab cavity. The large imaginary tunes effectively broaden the transverse resistance.

ESR

The standard vacuum chamber for the ESR has an elliptical cross-section with a 80 mm full width and a 36 mm vertical full height. Each vacuum component undergoes several iterations in impedance optimization. Three different codes: GdfidL [7], CST [8] and ECHO3D [9] are applied for the impedance modelling of the EIC vacuum components in time domain and frequency domain. While good agreements were reached among the codes in general, there were discrepancies found for some of the components. The cross-checking with different codes helped us to identify some bugs of the simulation code, proper set-up of the simulation, as well as defects in the 3D model [10]. Figure 3 presents an example of cross-checking the longitudinal wake potential for a 8 mm bunch length as calculated by the three codes for the ESR conventional type bellows,

indicating a discrepancy of the results from CST and that from the other two codes. Sources of such discrepancy are still under investigation.

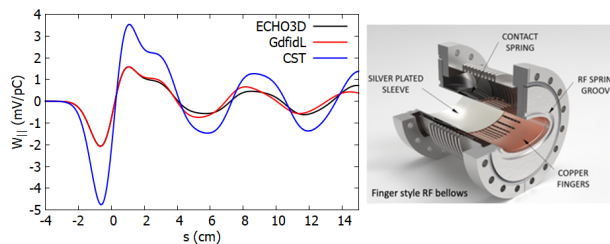


Figure 3: Comparison of the longitudinal wake potential as calculated by ECHO3D, GdfidL and CST, for the EIC conventional type bellows.

The main bending dipoles in the ESR consist of three segments each. To accelerate the electron beam at 5 GeV energy, the center dipole provides a reverse bend with small bending radius. At 10 GeV and 18 GeV all dipoles have the same bending direction. In Table 1, we list the ESR vacuum components that contribute to the beam induced effects, which are included into the total longitudinal ($W_{||,tot}$) and transverse dipole ($W_{yD,tot}$) and quadrupole wakefields for the particle tracking simulations. Based on the electron energy, the orbit will be shifted relative to the vacuum chamber center, predominantly in the arcs of the ESR. The longitudinal and transverse wakefields for the dipole chambers are calculated relative to the center of the vacuum chamber w/o horizontal shift. The CSR wakefield has been simulated using Demin Zhou’s CSRZ code [11] for two different magnet schemes, for the reverse bend at 5 GeV and for all dipoles have the same bending direction at 10 GeV and 18 GeV. The considered vacuum chamber for the CSR wakefield simulations has a rectangular cross-section with 80 mm x 36 mm geometric dimensions. The vacuum chamber surface is approximated by a 3018 m long copper pipe with a 18 mm vertical half-aperture and a resistivity of $\rho_e = 1.7 \times 10^{-8} \Omega\text{m}$.

Table 1: The list of the Vacuum Components that Contribute to the Beam Induced Effects Included into the Total Wakefield Simulations

Components	Abbreviation	Number
Bellows	BLW	350
Collimator Ramp ¹	CLM	16
Crab Cavity	CRBCVT	2
Beam Position Monitor ²	BPM	494
Gate Valve ²	GV	30
Stripline Kicker ²	SK	18
Main RF Cavity ²	CVT	23
Multipole Chamber Absorber	MPABS	292
Dipole Chamber Absorber	DPABS	250
Resistive Wall	RW	-
Coherent Synchrotron Radiation	CSR	-

¹ SKEKB design

² NSLS-II vacuum components with original apertures

The total longitudinal wakefield at 5 GeV and 10 GeV/18 GeV energies is shown in Fig. 4, while the transverse dipole wakefield is presented in Fig. 5. The main parameters for the beam dynamics simulations in the ESR are listed in Table 2.

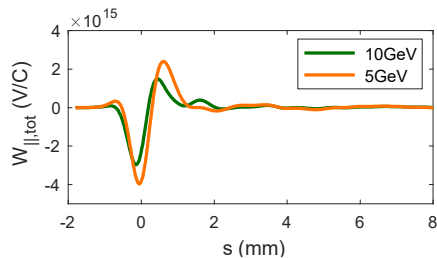


Figure 4: The total longitudinal wakefield simulated for a 0.3 mm bunch length at 5 GeV and 10/18 GeV energies.

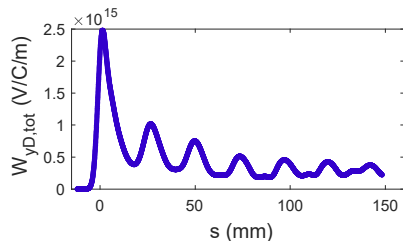


Figure 5: The total vertical dipole wakefield simulated for a 2 mm bunch length.

Table 2: The Main ESR Parameters for the Beam Dynamics Simulations

Energy	5 GeV	10 GeV
Average Current, I_{av} [A]	2.5	
Revolution Period, T_0 [μ s]	12.79	
Momentum Compaction, α	1.03×10^{-3}	
Harmonic Number, h	7560	
Energy Loss, U_0 [MeV]	1.3	3.52
RF Voltage, V_{RF} [MV]	12	24
Synchrotron Tune, ν_s	0.054	0.054
Damping Time, $\tau_{x,y}, \tau_s$ [ms]	100	50
Energy Spread, σ_δ	0.00068	0.00058
Bunch Length, σ_s [mm]	7.9	6.7

To estimate the longitudinal single-bunch effects, the energy spread and the bunch length dependence on the single-bunch current are studied using the TRANFT code [3] for two electron energies (Fig. 6). The microwave instability threshold current is $I_{th,5GeV} = 3$ mA at 5 GeV and $I_{th,10GeV} = 4$ mA at 10 GeV, those are higher than the required single-bunch current for stable operation, $I_0 = 2.2$ mA. These estimates we made without including the IBS effect. The Transverse Mode Coupling Instability (TMCI) threshold is higher than the observed one, since both the transverse dipole and the longitudinal total wakefields were using simultaneously for a particle tracking simulations.

Mitigating beam-induced heating is another challenging task in EIC, especially in the ESR, where the average beam current is $I_{av} = 2.5$ A within $M = 1160$ bunches and with the bunch length of ~ 7 mm. The beam-induced heating is estimated for each individual component and it includes power loss calculations and the thermal simulations. Some of the components will require water cooling or changes in their design. R&D projects are expected for some of the key components including bellows, interaction region (IR) chamber, collimation system, BPMs, and etc.

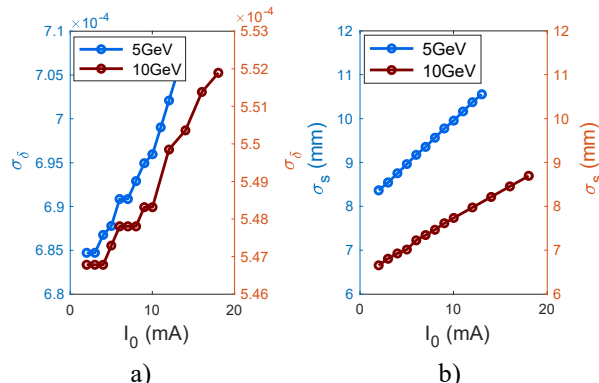


Figure 6: a) Energy spread σ_δ and b) bunch length σ_s as a function as a function of single-bunch current I_0 at 5 GeV and 10 GeV.

CONCLUSION

Currently we have rough design of the main vacuum components. As the first step we use the geometric impedances of the vacuum chamber components simulated for NSLS-II and Super KEKB. The impedance budget will be updated next with more impedance data available for the optimized ESR vacuum components.

ACKNOWLEDGEMENTS

We would like to thank Demin Zhou for introduction to the CSRZ code, configuring it for different lattices and useful discussions on the longitudinal beam dynamics.

REFERENCES

- [1] J. Adam *et al.*, “EIC Conceptual Design Report”, BNL, Upton, NY, USA, Rep. EIC CDR, 2021.
- [2] BNL Staff, “RHIC Conceptual Design Report”, BNL, Upton, NY, USA, Rep. BNL 52195, 1989.
- [3] M. Blaskiewicz, “A Multipurpose Coherent Instability Simulation Code”, in *Proc. 22nd Particle Accelerator Conf. (PAC'07)*, Albuquerque, NM, USA, Jun. 2007, paper THPAS090, pp. 3690-3692.
- [4] S. Verdú-Andrés *et al.*, “A Beam Screen to Prepare the RHIC Vacuum Chamber for EIC Hadron Beams: Requirements and Conceptual Design”, presented at IPAC'21, Campinas, Brazil, May 2021, paper TUPAB260, this conference.
- [5] B. Angerth *et al.*, “The LHC Beam Screen - Specification and Design”, in *Proc. 4th European Particle Accelerator Conf. (EPAC'94)*, London, UK, Jun.-Jul. 1994, pp. 208-211.
- [6] C. Garion, V. Baglin, and R. Kersevan, “Preliminary Design of the High-Luminosity LHC Beam Screen with Shielding”,

in *Proc. 6th Int. Particle Accelerator Conf. (IPAC'15)*,
Richmond, VA, USA, May 2015, pp. 60-63.
doi:10.18429/JACoW-IPAC2015-MOBD1

- [7] W. Bruns, <http://www.gdfid1.de>
- [8] CST Particle Studio, <http://www.cst.com>
- [9] I. Zagorodnov, "Indirect methods for wake potential integration", *Phys. Rev. ST Accel. Beams*, vol. 9, p. 102002, 2006. doi:10.1103/PhysRevSTAB.9.102002
- [10] G. Wang, M. Blaskiewicz, A. Blednykh, and M. P. Sangroula, "Studies of the Short-Range Wakefields for the Electron Storage Ring in the Electron Ion Collider", presented at the 12th Int. Particle Accelerator Conf. (IPAC'21), Campinas, Brazil, May 2021, paper WEPAB032, this conference.
- [11] D. Zhou *et al.*, "Calculation of Coherent Synchrotron Radiation Impedance for a Beam Moving in a Curved Trajectory", *Jpn. J. Appl. Phys.*, vol. 51, p. 016401, 2012.
doi:10.1143/JJAP.51.016401